A Procedure for Designing EMI Filters for AC Line Applications

Fu-Yuan Shih, Dan Y. Chen, *Senior Member, IEEE,* Yan-Pei Wu, and Yie-Tone Chen, *Member, IEEE*

***Abstract*— A procedure for designing ac line EMI filters is presented. This procedure is based on the analysis of conducted EMI problems and the use of a noise separator. Design examples are given, and results are experimentally verified.**

I. Introduction

FIXING conducted electromagnetic interference (EMI) problems is not an exact science. It normally involves a cut-and-trial process for a designer to come up with a proper filter design. As such, designing a filter is a time-consuming process for beginning engineers as well as for experienced engineers when they face new design circumstances.

In this paper, a procedure for designing EMI filters for ac line-powered equipment will be presented. This procedure is based on the analysis of conducted EMI problems and the use of an EMI diagnostic tool, noise separator, developed recently [1]. The noise separator, constructed from a radio-frequency power splitter, can be used to separate differential-mode (DM) and common-mode (CM) noise. This greatly simplifies the filter design process. In the paper, a review of conducted EMI problems will be given first. Factors affecting EMI performance and issues of filter design will be described. From the discussion, a practical approach to designing EMI filters emerges and a design procedure will be proposed. Numerical examples will be given to illustrate the design procedure and the results are experimentally verified.

II. EMI Measurement and Filter Noise Equivalent Circuit

A brief review of conducted EMI measurement is important to the discussion of filter design to be described later. Fig. 1 shows the setup diagram of a typical conducted EMI measurement. The line impedance stabilizing network (LISN), required in the measurement, contains inductors, capacitors, and 50 Ω resistors. For power line frequency, the inductors are essentially shorted, the capacitors are essentially open, and the power passes through to supply the equipment under test. For EMI noise frequency, the inductors are essentially open

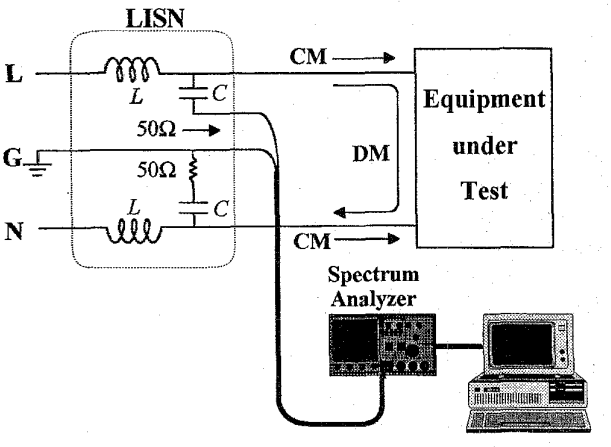

Fig. 1. Test setup for conducted EMI measurement.

circuit, the capacitors are essentially shorted and the noise sees 50 Ω resistors. The noise voltage measured across the 50 W input impedance of a spectrum analyzer, expressed in frequency ranging from 10 KHz to 30 MHz for VDE limit and from 450 KHz to 30 MHz for FCC limit, is by definition the conducted EMI.

The noise voltage, measured from the 50 Ω resistors contains both common-mode (CM) noise and differential-mode (DM) noise. Each mode of noise is dealt with by the respective section of an EMI filter. Fig. 2(a) shows a commonly used filter network topology, and Fig. 2(b) and (c) shows, respectively, the equivalent circuit of the CM section and the DM section of the filter. Referring to Fig. 2(b) and (c), it is noticed that some elements of the filter affect DM (or CM) noise only and some affect both DM and CM noise. The capacitors C_{X1} and C_{X2} affect DM noise only. An ideal common-mode choke L_C affects CM noise only, but the leakage inductance $L_{leakage}$ between the two windings of L_C affects DM noise. C_y suppresses both CM noise and DM noise, but its effect on DM noise suppression is practically very little because of the relatively large value of C_{X2}. Similarly, L_D suppresses both DM noise and CM noise, but its effect on CM noise is practically very little because of the relatively large value of L_C.

The two modes of noise contribute to the total EMI noise. It has been reported recently that the two modes of noise can be deciphered experimentally from the total noise by using a noise separator. The noise separator is capable of selectively providing at least 50 dB rejection to either DM or CM noise from a total noise. It is to be used in the filter design proposed in the present paper.

Manuscript received September 24, 1995; revised August 4, 1995.

F.-Y. Shih and Y.-P. Wu are with the Department of Electrical Engineering, National Taiwan University, Taipei, Taiwan.

D. Y. Chen is with the Department of Electrical Engineering, Virginia Polytechnic Institute and State University, Blacksburg, VA 24061 USA.

Y.-T. Chen is with the Department of Electrical Engineering, National Yunlin Institute of Technology, Tou-Liu City, Taiwan.

Publisher Item Identifier S 0885-8993(96)00586-8.

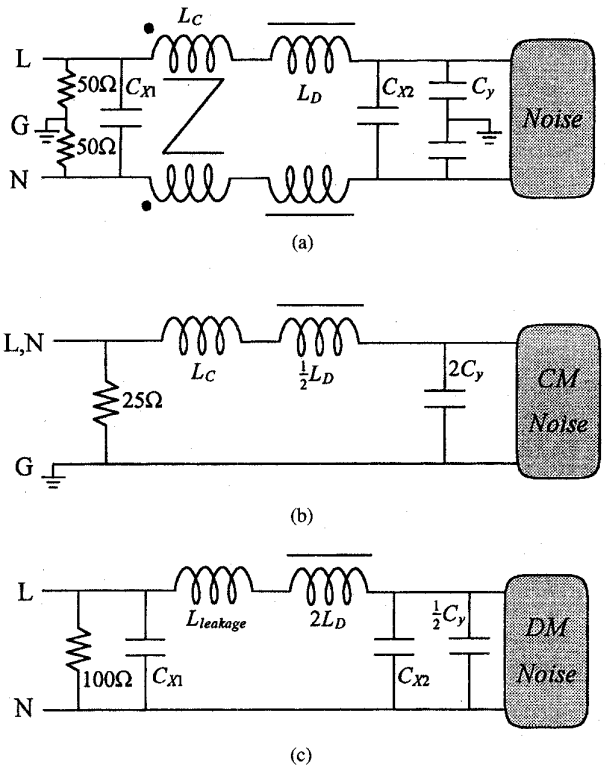

Fig. 2. (a) Typical EMI filter topology. (b) CM noise equivalent circuit of (a). (c) DM noise equivalent circuit of (a).

III. Difficulties of Predicting Conducted EMI Performance

There are several reasons, both theoretical and practical, why it is difficult to predict conducted EMI performances. They are described in the following. From the difficulties described, a practical procedure for designing the EMI filter emerges and will be described in Section IV.

1) DM and CM noises are coupled through different paths to the measured EMI. Equipment package and component layout all affect the coupling paths. but the effects are very difficult to quantify. Often, a seemingly small change in layout could lead to significant change in EMI performance.

2) The effectiveness of an EMI filter depends not only on the filter itself but also on the noise source impedance [2]. Fig. 3(a) shows a typical power converter and the related input waveforms. The equivalent models of CM and DM noise source impedances of Fig. 3(a) are depicted in Fig. 3(b) and (c), respectively. For CM noise, the source is modeled by a current source in parallel with a high source impedance Z_P. For DM noise, the source is modeled by a voltage source in series with a low impedance or a current source in parallel with a high impedance dependent on the state of the input rectifier diodes [2]. When two of the rectifier diodes are conducting, the noise source is modeled by a voltage source in series with low-impedance source Z_S, and when all of the four diodes are cut off, the noise is modeled by a current source in parallel with a high-impedance Z_P. The DM equivalent circuit therefore fluctuates between these two model at two times the line frequency. Z_S is associated with wire inductance and resistance,

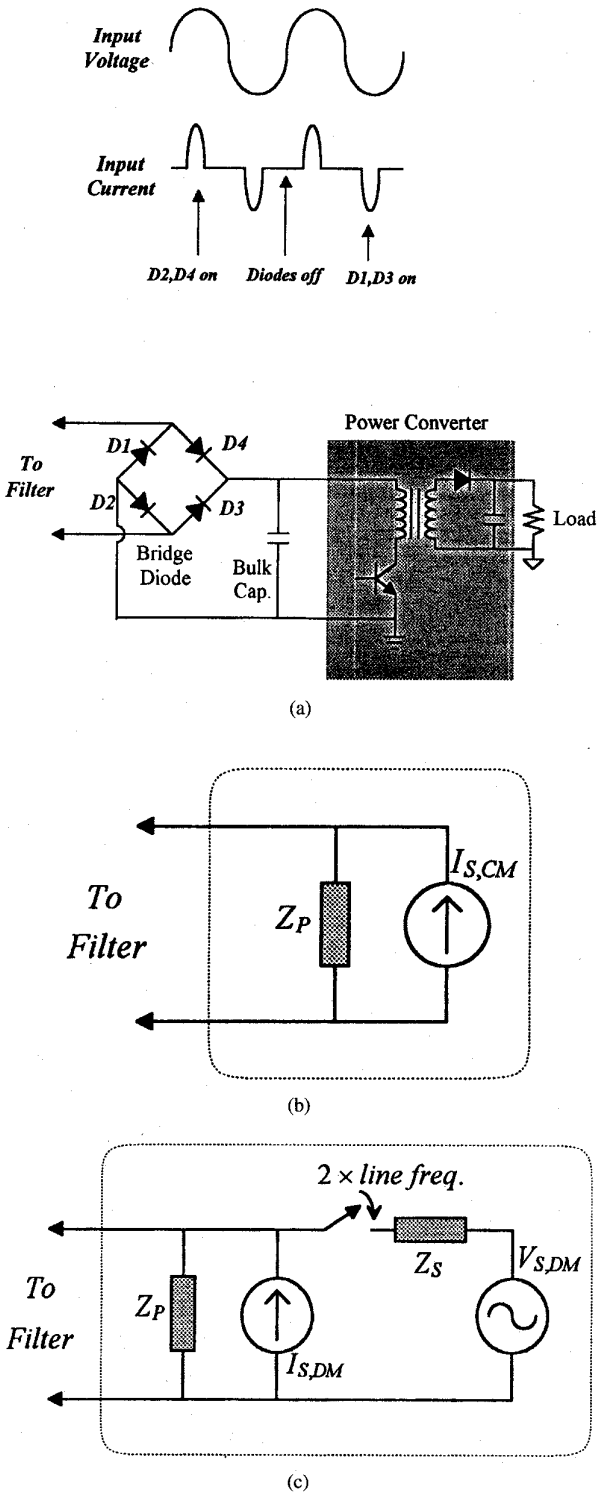

Fig. 3. (a) Typical power converter and the related input waveforms. (b) Equivalent model of CM noise source of (a). (c) Equivalent model of DM noise source of (a).

and Z_P is associated with diode parasitic capacitance. These source impedances depend on parasitic parameters and are therefore package-dependent. Although the source impedances can be measured, this is practically difficult [2].

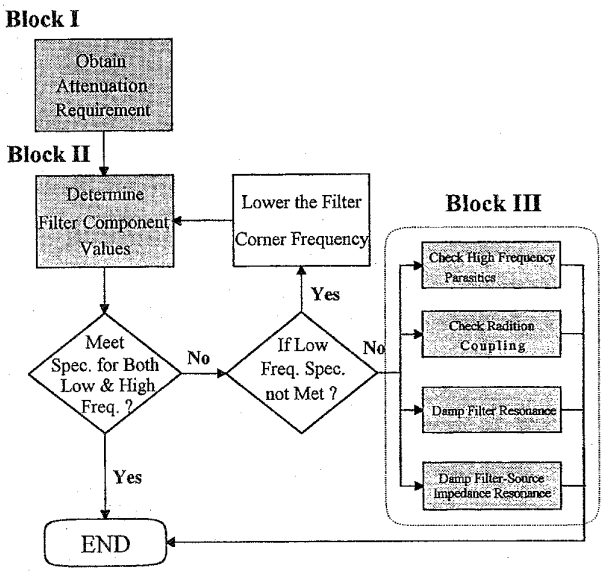

Fig. 4. Design flow chart of EMI filters.

3) Beyond a certain frequency, the effects of parasitic elements start to surface. This frequency is the dividing line between "high frequency" and "low frequency" used in the paper here. High-frequency effects include permeability reduction of choke core, parasitic capacitance effect of the inductor, and the parasitic inductance effect of filter capacitors. Besides the effects of parasitic elements, radiation coupling and source impedance-filter capacitor resonance [4] could also affect high-frequency EMI performance. These effects, however, are difficult to predict without experiments.

IV. Practical Approach to Designing EMI Filters

From the discussion of the last section, it is clear that it is extremely difficult to analytically arrive at an EMI filter design. A practical approach is proposed here to deal with the difficult issue. This approach is based on the following three understandings:

1) Base-line (i.e., without filter) EMI noise must be provided to filter designer. This information is obtained either through past history or actual measurement. For products without past history, it is difficult to estimate the base-line EMI noise, and the information must be obtained by measurement. The noise separator mentioned earlier will be used in obtaining the base-line level for both the CM and DM noise.

2) Although, in general, noise source impedance affects filter attenuation, it can be proved that as long as the filter elements are properly arranged and sized, source impedance has little effect. Therefore, analytical design of the filter is possible without knowing exactly the source impedance values. The detailed explanations are given in Section IV-B.

3) Because it is difficult to predict high-frequency performance at the stage of filter design, the focus of the filter design procedure is to meet the low-frequency specification. After the filter is designed and built, high-frequency performance can be tuned if necessary.

A. Design Flow Chart

Based on the preceding discussion, a flow chart for EMI filter design is proposed in Fig. 4. In Block I of the chart, filter attenuation requirement is obtained first. This involves the use of a noise separator for base-line noise measurement for both CM and DM noise. Based on the information obtained in Block I, component values of an EMI filter will be determined in Block II, mainly to meet low-frequency specification. Theoretically speaking, the filter design obtained in Block II should meet both the low-frequency and the high-frequency specification. However, many high-frequency effects, which are difficult to deal with at the design stage of the filter, may cause the violation of high-frequency design specification. Block III provides a list of possible causes of such violation, which include high-frequency parasitic effects of filter components, radiation coupling problems, filter source-impedance resonance, and filter underdamped resonance. The main focus of the present paper is on Blocks I and II. Block III is beyond the scope of the paper.

B. Basis of Determining Filter Component Values

1) Common Mode: From Figs. 2(b) and 3(b), the CM noise equivalent circuit can be represented by Fig. 5(a). If the impedance conditions indicated in the figure are met, then the filter attenuation by the transfer function $V_{S,CM}/V_{0,CM}$ is shown in Fig. 5(c). In the figure, the filter attenuation is defined as V_{LISN}(without filter)/V_{LISN}(with filter). Notice that the Reciprocity Theorem (open circuit voltage ratio is equal to short circuit reverse current ratio) is used from Fig. 5(b) to (c). The filter attenuation is therefore determined by L_{CM} $(= L_C + L_D/2)$ and C_{CM} $(= 2C_y)$ and is independent of source impedances. Fig. 5(d) shows the plot of CM noise attenuation versus frequency. Normally, $L_C \gg \frac{1}{2}L_D$ and the corner frequency $f_{R,CM}$ is mainly determined by L_C and C_y values. This figure will be used in Section V for the determination of CM filter component values. It is noted that the impedance inequalities indicated in Fig. 5 are normally met in typical filters [3].

2) Differential Mode: It was shown in Fig. 3(c) that the source impedance of the DM noise for an ac line-powered circuit can be either "high" or "low," depending on the conducting state of the rectifier diodes. Fig. 6 shows the two noise equivalent circuits and the graphical explanation leading to the derivation of filter attenuation of DM filter. When the rectifier diodes are off, a high-Z model for the noise source is used and the equivalent circuit is shown in Fig. 6(a). When diodes are on, the low-Z model shown in Fig. 6(b) is used. If the impedance conditions indicated in the figure are met, then the filter attenuation can be approximated by the transfer function $V_{S,DM}/V_{o,DM}$ of Fig. 6(e) and (f). Notice that from Fig. 6(c) to (e), the Reciprocity Theorem is used. DM equivalent circuit fluctuates between the two models every 2×line frequency; it is difficult to distinguish the individual contribution to the total DM noise. However, if $C_{X1} = C_{X2} = C_{DM}$, the total filter attenuation to DM noise is determined by L_{DM} $(= 2 \cdot L_D + L_{leakage})$ and C_{DM} alone. The attenuation is therefore approximated by a 40dB/dec-

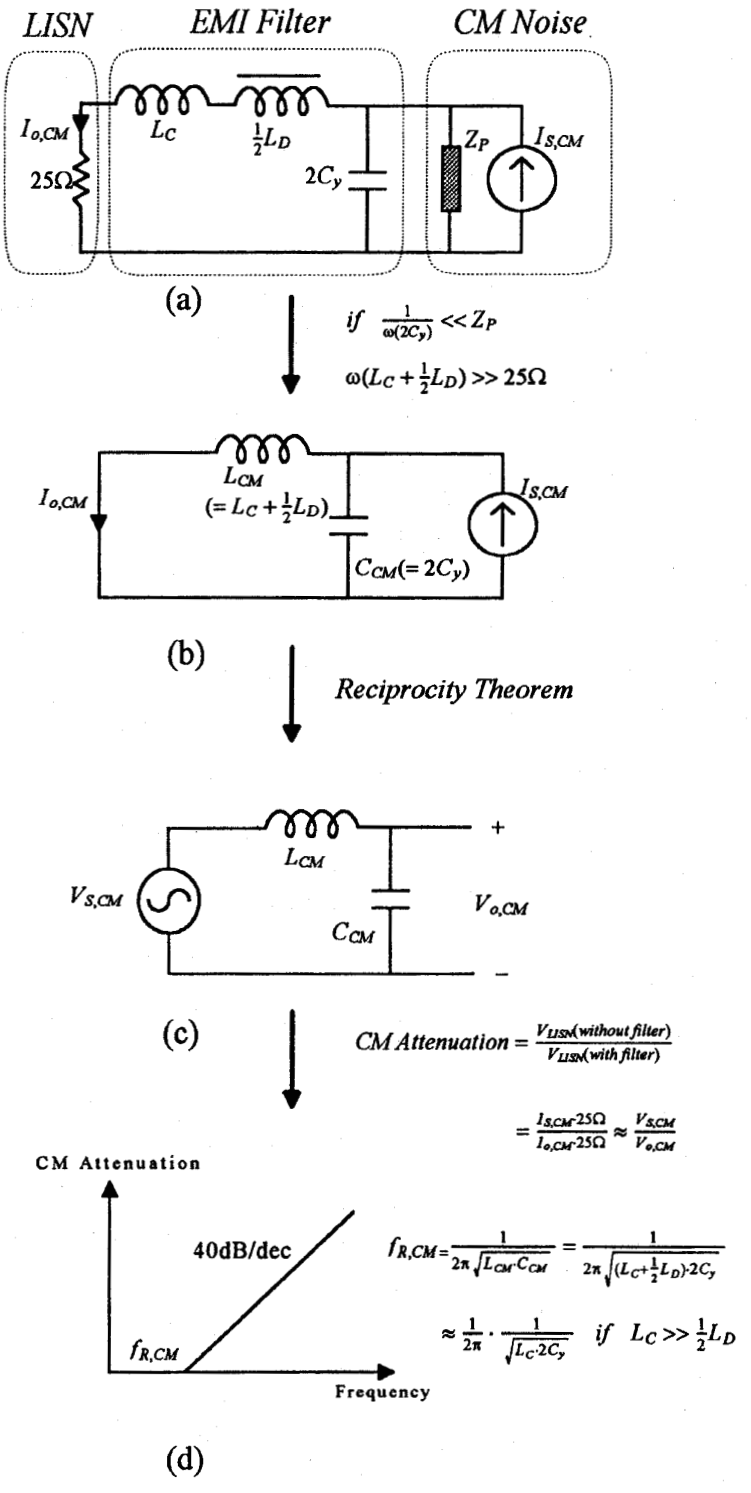

Fig. 5. Equivalent circuits for the derivation of CM filter attenuation. (a) CM equivalent circuit. (b) Equivalent circuit of (a) if $\frac{1}{\omega(2C_y)} \ll Z_p$ and $\omega(L_C + \frac{1}{2}L_D) \gg 25\ \Omega$. (c) Equivalent circuit of (b) by using *Reciprocity Theorem*. (d) Filter attenuation for common-mode noise.

slope line going through $L_{DM}C_{DM}$ resonance frequency, as shown in Fig. 6(g). Notice that there is no peaking effect at the resonance in Figs. 5(d) and 6(g). In practical filters there is usually enough damping that at resonant frequency there is no peaking.This figure will be used in Section V for the determination of DM filter component values. It is also noted that the inequalities indicated in Fig. 6 are met for typical filters [3].

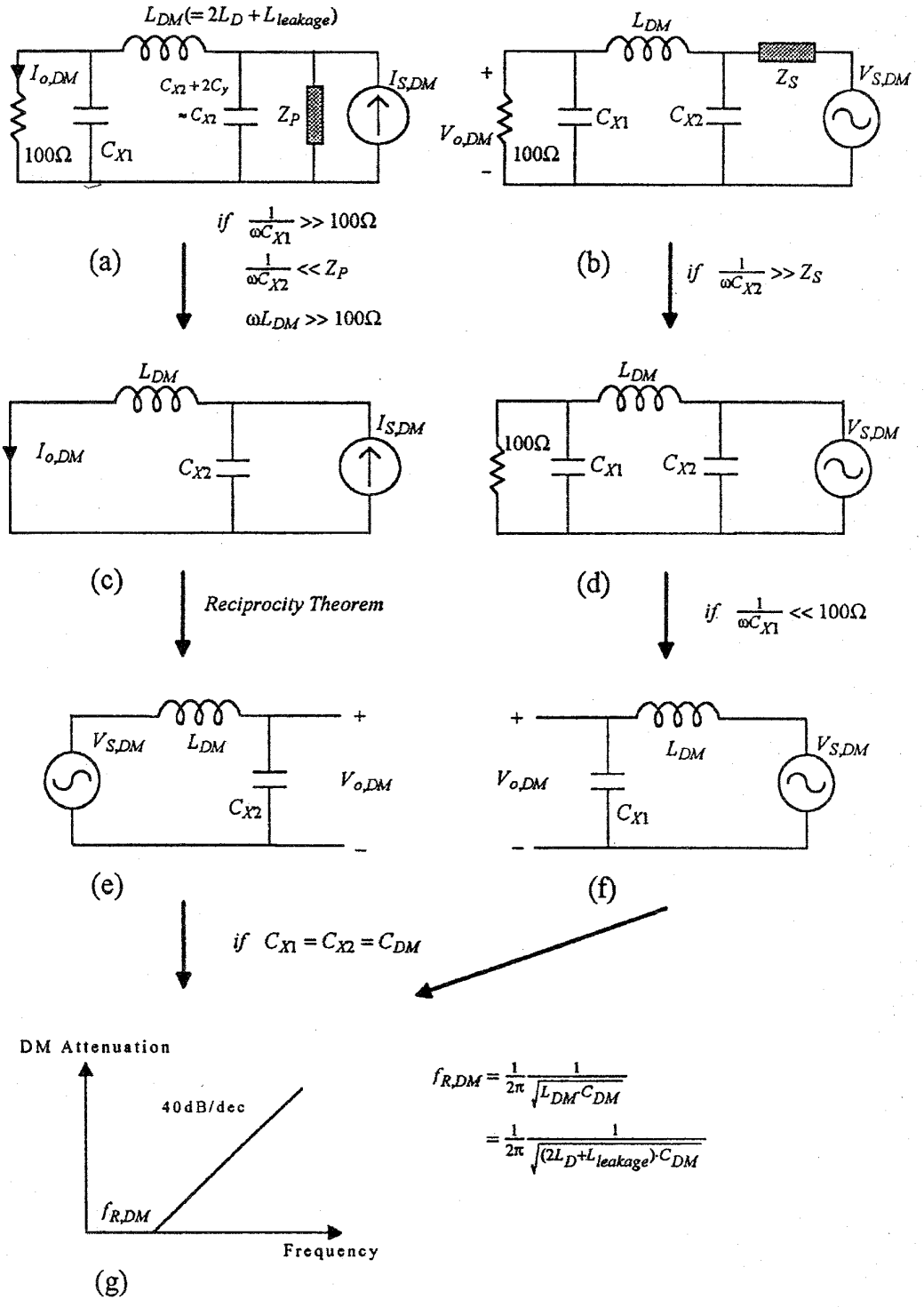

Fig. 6. Equivalent circuits for the derivation of DM filter attenuation. (a) DM equivalent circuit when rectifier diodes are conducting. (b) DM equivalent circuit when rectifier diodes are not conducting. (c) Equivalent circuit of (a) if $1/\omega C_{X1} \gg 100\ \Omega, 1/\omega C_{X2} \ll Z_P$ and $\omega L_{DM} \gg 100\ \Omega$. (d) Equivalent circuit of (b) if $1/\omega C_{X2} \gg Z_s$. (e) Equivalent circuit of (c) by using *Reciprocity Theorem*. (f) Equivalent circuit of (d) if $1/\omega C_{X1} \ll 100\ \Omega$. (g) Filter attenuation for differential-mode noise.

V. Design Procedure for EMI Filters

Based on the discussion given above, a procedure for filter design is proposed in the following. A commonly used filter topology shown in Fig. 2(a) is used for illustration. It is noted that the main objective of this procedure is to meet the low-frequency specification. Once designed and built, modification

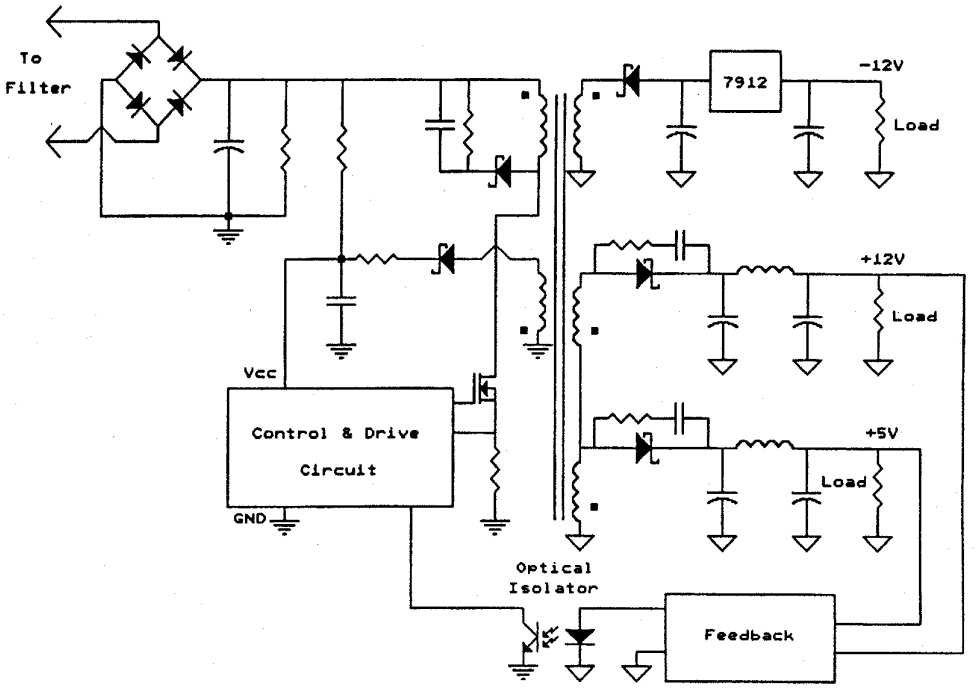

(a)

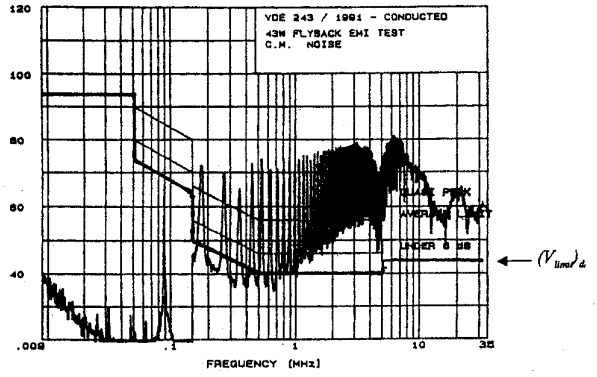

(b)

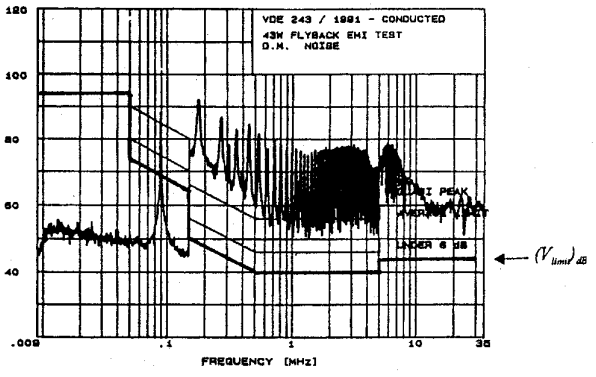

(c)

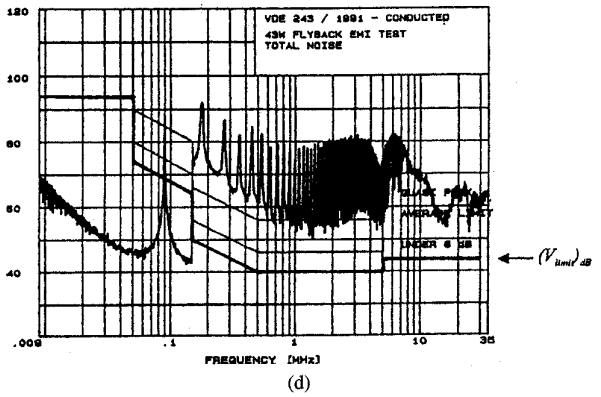

(d)

Fig. 7. (a) Circuit diagram of a 43 W flyback switching power supply. (b) Base-line CM noise of (a). (c) Base-line DM noise of (a). (d) Base-line total noise of (a).

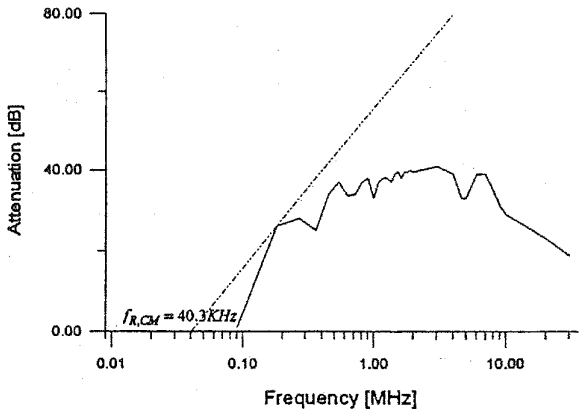

(a)

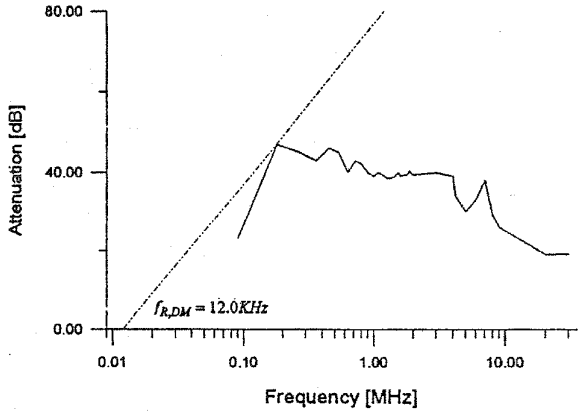

(b)

Fig. 8. (a) CM attenuation requirement for Example 1: ——— CM attentuation req. $(V_{req,CM})_{dB}$; – ·· – ·· – 40 dB/dec-slope line. (b) DM attenuation requirement for Example 1: ——— DM attentuation req. $(V_{req,DM})_{dB}$; – ·· – ·· – 40 dB/dec-slope line.

may be needed to meet the high-frequency specification, but this modification is beyond the scope of the paper.

A. Design Procedure

Step 1: Measure base-line (i.e., without filter) common-mode EMI noise V_{CM} and differential-mode EMI noise V_{DM} using a noise separator.

Step 2: Determine CM attenuation requirement $V_{\text{req},CM}$ and DM attenuation requirement $V_{\text{req},DM}$

$$(V_{\text{req},CM})_{dB} = (V_{CM})_{dB} - (V_{\text{Limit}})_{dB} + 3dB$$
$$(V_{\text{req},DM})_{dB} = (V_{DM})_{dB} - (V_{\text{Limit}})_{dB} + 3dB$$

where $(V_{CM})_{dB}$ and $(V_{DM})_{dB}$ are obtained from *Step 1* and $(V_{\text{Limit}})_{dB}$ is the conducted EMI limit specified by FCC or VDE. A "+3dB" is needed because DM or CM measurement using the Noise Separator is 3dB above the actual value [1].

Step 3: Determine filter corner frequencies.

Based on Fig. 5(d), filter corner frequency $f_{R,CM}$ can be obtained by drawing a 40dB/dec-slope line that is tangent to the $(V_{\text{req},CM})_{dB}$ obtained in *Step 2*. The horizontal intercept of the line determines the CM filter corner frequency $f_{R,CM}$ Similarly, DM corner frequency $f_{R,DM}$ can also be determined from $(V_{\text{req},DM})_{dB}$.

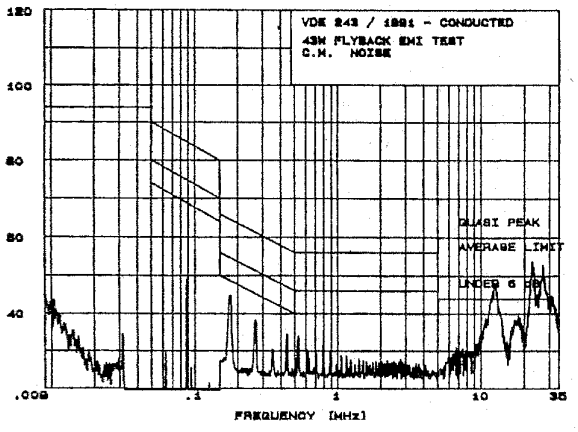

(a)

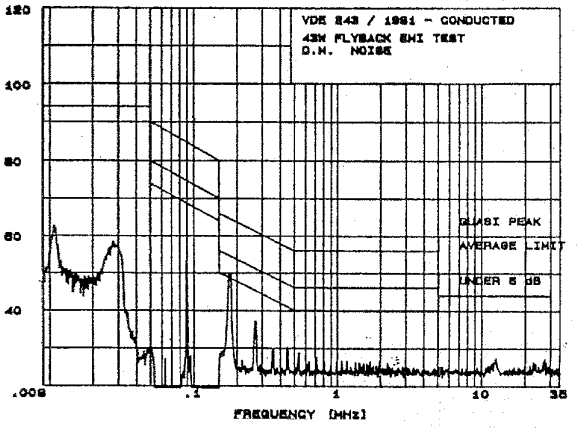

(b)

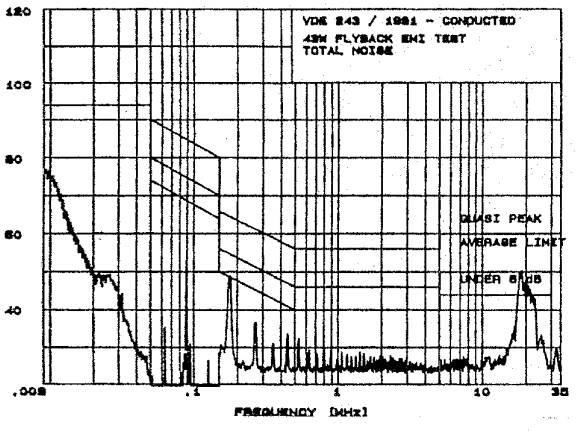

(c)

Fig. 9. (a) Measured CM noise for Example 1 when *Filter A* is used. (b) Measured DM noise for Example 1 when *Filter A* is used. (c) Measured total noise for Example 1 when *Filter A* is used.

Step 4: Determine filter component values.

a) CM component L_C and C_y: Since there is a safety leakage current requirement, C_y is normally limited to 3300 pF for 60 Hz operation. L_C and $2C_y$ should have a resonant frequency of $f_{R,CM}$ obtained in Step 3.

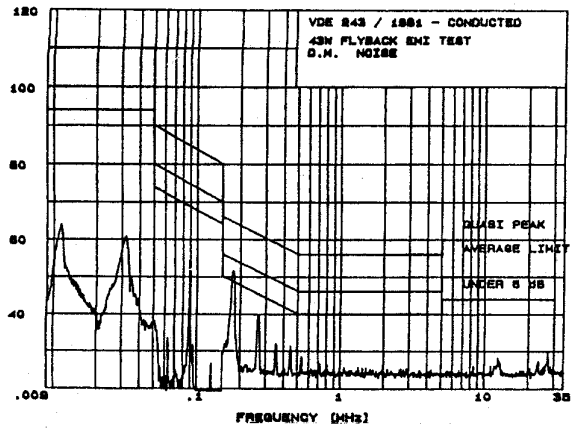

Fig. 10. DM noise for Example 1 when *Filter B* is used.

Therefore

$$L_C = \left(\frac{1}{2\pi \cdot f_{R,CM}}\right)^2 \cdot \frac{1}{2 \cdot C_y}. \quad (1)$$

b) DM component L_D, C_{X1} and C_{X2}: Based on the description given in Section IV-B, C_{X1} and C_{X2} are selected to be the same value C_{DM} and are related to L_{DM} through corner frequency $(f_{R,DM})$ requirement as shown by (2)

$$C_{X1} = C_{X2} = C_{DM} = \left(\frac{1}{2\pi \cdot f_{R,DM}}\right)^2 \cdot \frac{1}{L_{DM}}. \quad (2)$$

In (2), $f_{R,DM}$ value has been found in Step 3. C_{X1}, C_{X2}, and L_{DM} are unknowns. There exists some degree of freedom for trade-off. The larger the L_{DM} value selected, the smaller the C_{X1}, C_{X2} are needed, and vice versa. In choosing the C_Xs' value, input filter stability problem must also be considered [5].

Since the leakage inductance of a CM choke can be utilized as a DM choke, separate DM chokes may not be needed in some cases. Practically, L_{leakage} is generally in the range of 0.5–2% of the L_C value.

B. Design Examples

Two design examples are given below to illustrate the design steps described above. Filter topology shown in Fig. 2(a) is used. One example is for the flyback converter power supply, and the other is for the forward converter power supply. The results of both examples are verified experimentally.

Example 1: Design an EMI filter for an off-line (90–260 V) flyback converter switching power supply (90 KHz, 43 W output), as shown in Fig. 7(a), to meet a VDE limit. For proper margin, under 6 dB limit is used in the design [see Fig. 7(b)].

Step 1: The base-line CM noise V_{CM} and the base-line DM noise V_{DM} of the tested circuit, measured by using a noise separator, is shown in Fig. 7(b) and (c), respectively. Fig. 7(d) shows the total noise V_{Total} of the tested circuit.

Step 2: The CM attenuation requirement $(V_{req,CM})_{dB}$ and the DM attenuation requirement $(V_{req,DM})_{dB}$ are plotted in log-log scale, as shown in Fig. 8(a) and (b). The line labeled "Under 6 dB" is used as the $(V_{limit})_{dB}$.

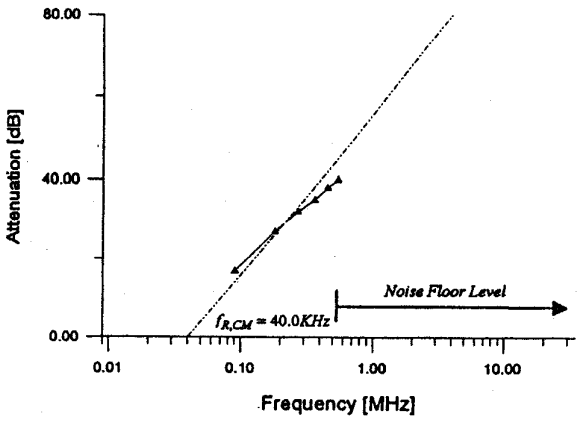

(a)

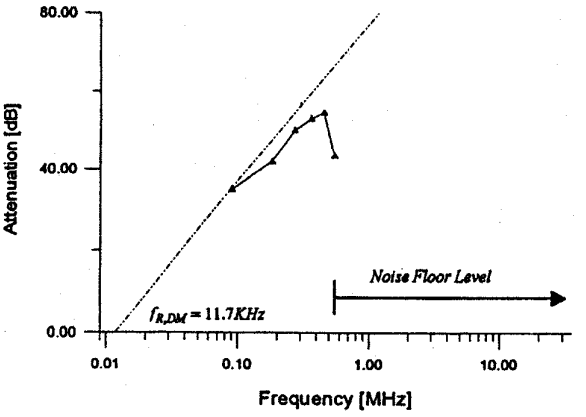

(b)

Fig. 11. Comparisons of the actual filter performance and the predicted performance of Example 1 when *Filter A* is used. (a) CM attenuation. (b) DM attenuation. ——▲—— experimental attentuation; – ·· – ·· – theoretical attentuation.

Step 3: From Fig. 8(a) and (b), $f_{R,CM} = 40.3$ KHz and $f_{R,DM} = 12.0$ KHz

Step 4a): Use C_y =3300 pF, calculate L_C according to (1)

$$L_C = \left[\frac{1}{2\pi \times (40.3 \times 10^3)}\right]^2 \cdot \frac{1}{2 \cdot 3300 \times 10^{-12}} = 2.36\,\text{mH}.$$

Select $L_C = 2.4$ mH, and the leakage inductance $L_{\text{leakage}} = 36\ \mu$H can be obtained by measurement.

Step 4b): Using $f_{R,DM} = 12.0$ KHz in (2), there are infinite sets of solution for L_{DM} and C_{DM}. Three sets of solution are listed for discussion in the following:

1) Use the leakage inductance as the DM choke. Since $L_{DM} = L_{\text{leakage}} = 36\,\mu$H, then C_{DM} $(= C_{X1} = C_{X2}) = 4.75\,\mu$F, which is an impractical value for line-voltage rated filter capacitor. The physical volume of such a capacitor is much too bulky.
2) If C_{DM} are chosen to be 0.47 μF, a commonly available filter capacitor value, then $L_{DM} = 374\,\mu$H and $L_D = L_{DM} - L_{leakage}/2 = 169\,\mu$H, a practical inductance value. Select $L_D = 180\,\mu$H.
3) If $C_{DM} = 0.22\,\mu$F, then $L_{DM} = 800\,\mu$H and $L_D = 382\,\mu$H, a practical value also. Select $L_D = 380\,\mu$H.

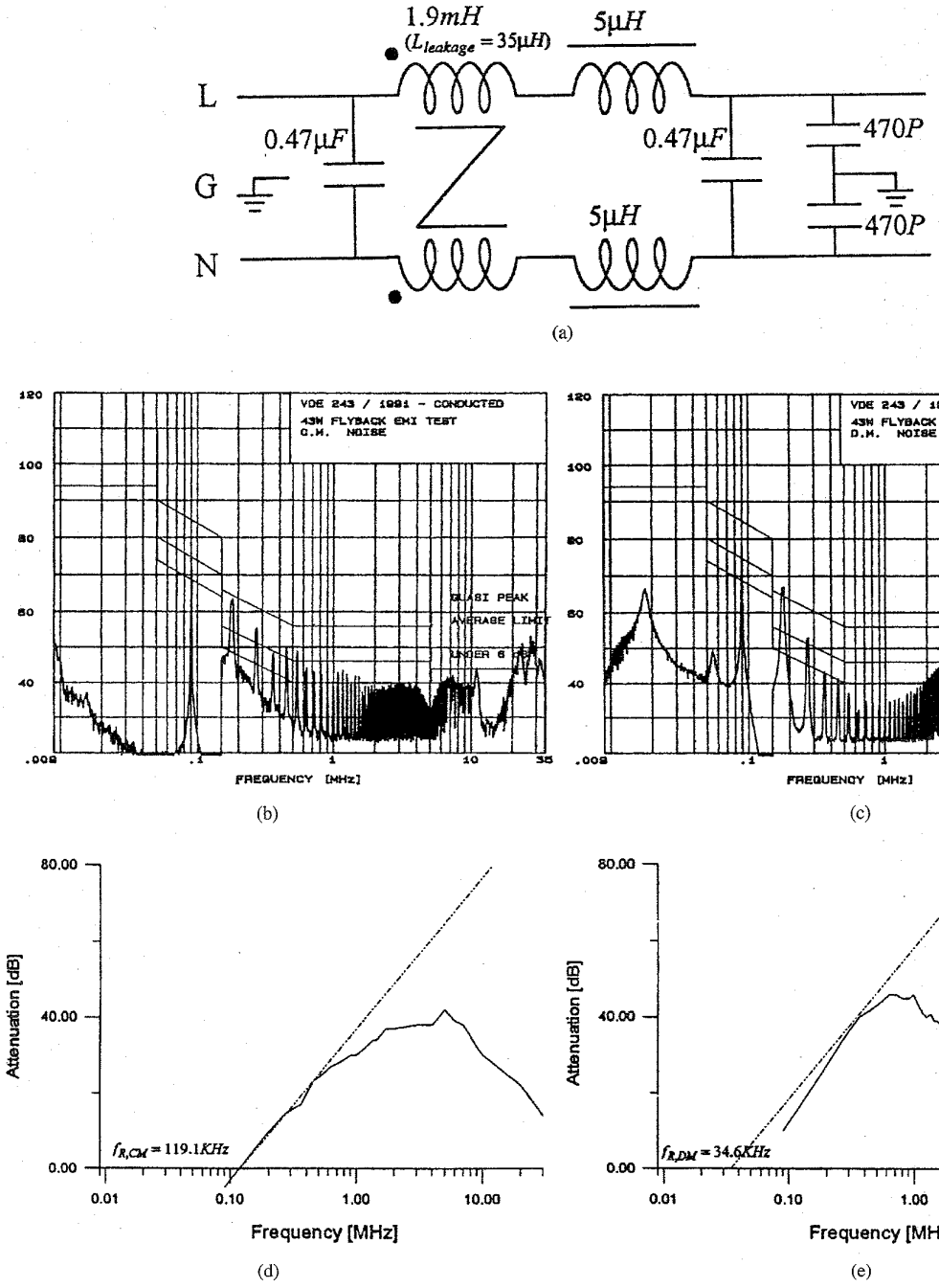

Fig. 12. (a) A smaller filter used to compare the actual filter performance and the predicted performance. (b) Measured CM noise for Example 1 when the filter shown in (a) is used. (c) Measured DM noise for Example 1 when the filter shown in (a) is used. (d) CM attenuation comparison of the actual filter performance and the predicted performance of Example 1 when the filter shown in (a) is used. (e) DM attenuation comparison of the actual filter performance and the predicted performance of Example 1 when the filter shown in (a) is used. —— experimental attentuation; —·—·— theoretical attentuation.

From the procedure, two filter designs were obtained

$$\textit{Filter A: } L_C = 2.4\,\text{mH}\ (L_{leakage} = 36\,\mu\text{H}), L_D = 180\,\mu\text{H}, \quad C_{X1} = C_{X2} = 0.47\,\mu\text{F}, C_y = 3300\,\text{pF}.$$

$$\textit{Filter B: } L_C = 2.4\,\text{mH}\ (L_{leakage} = 36\,\mu\text{H}), L_D = 380\,\mu\text{H}, \quad C_{X1} = C_{X2} = 0.22\,\mu\text{F}, C_y = 3300\,\text{pF}.$$

Discussion: Both sets of filter design were constructed and tested. Fig. 9 shows the conducted EMI test for the power supply using *Filter A*. It can be seen from the figure, *Filter A* meets the low-frequency design goal, which is the main focus of the paper. Around 20 MHz, the emission exceeds the limit. It was observed that the emission around 20 MHz was caused by radiation coupling. By rearranging the wiring between the EMI filter and the power supply, the problem was

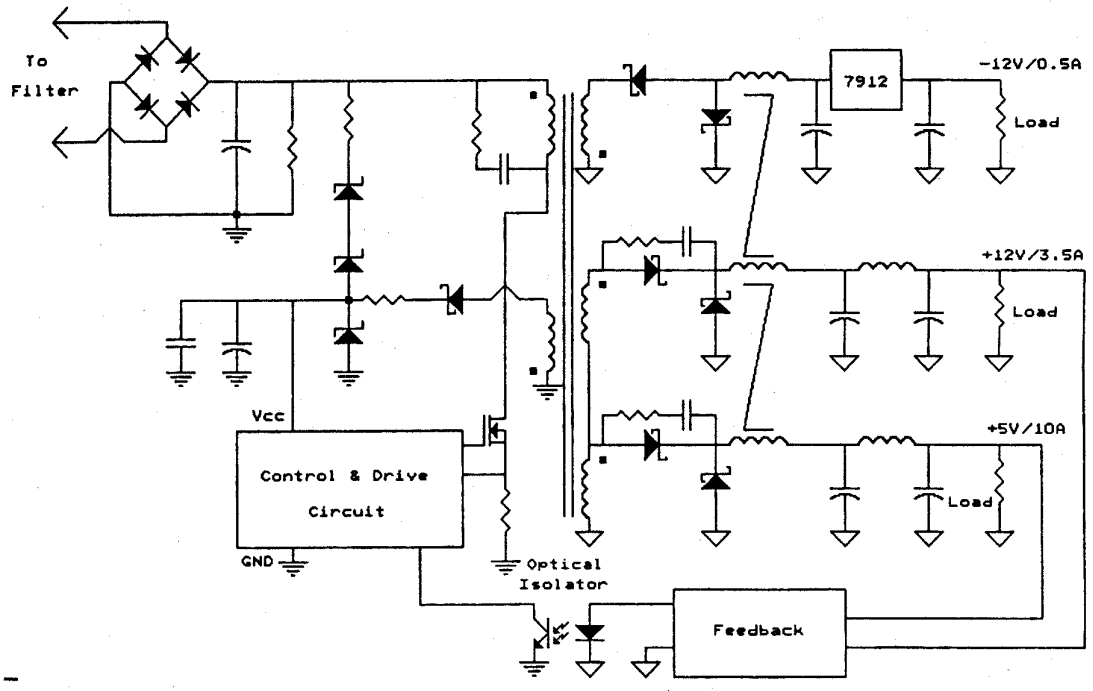

(a)

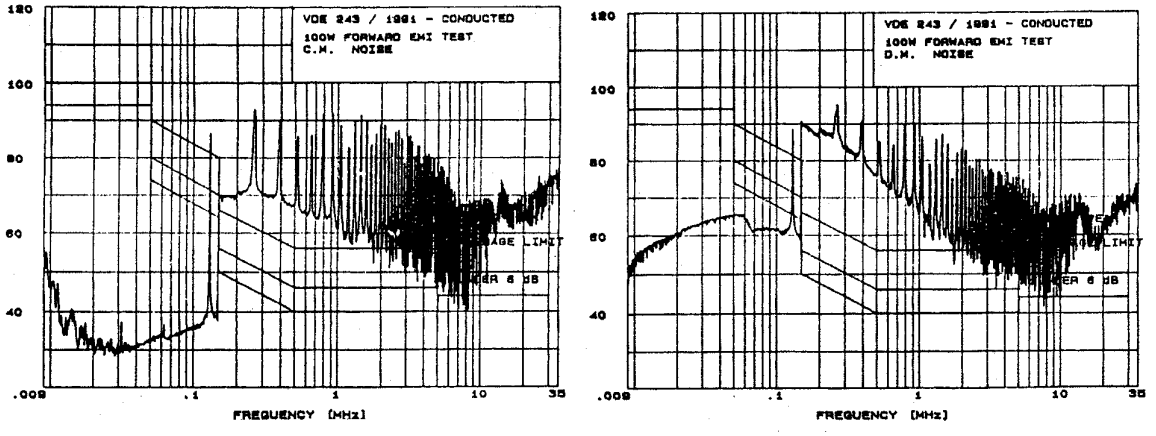

(b)

(c)

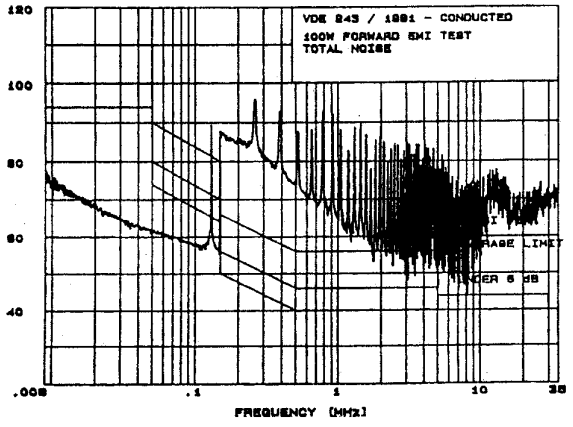

(d)

Fig. 13. (a) Circuit diagram of a 100 W forward switching power supply. (b) Base-line CM noise of (a). (c) Base-line DM noise of (a). (d) Base-line total noise of (a).

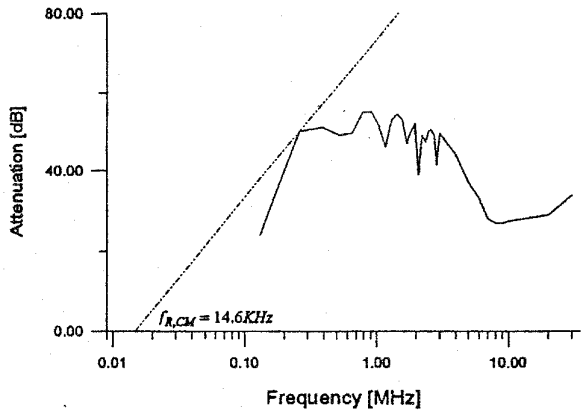

(a)

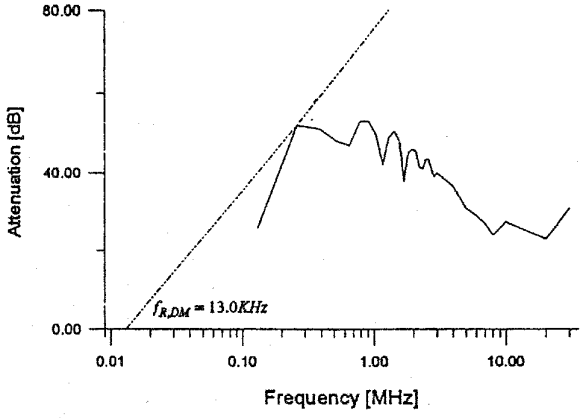

(b)

Fig. 14. (a) CM attenuation requirement for Example 2: ——— CM attentuation req. $(V_{req,CM})_{dB}$; —·—·— 40 dB/dec-slope line. (b) DM attenuation requirement for Example 2: ——— DM attentuation req. $(V_{req,DM})_{dB}$; —·—·— 40 dB/dec-slope line.

eliminated. Test results for *Filter B* show similar results and will not be repeated except for DM emission. Fig. 10 shows the DM emission (for *Filter B*), which is essentially the same as the DM emission for *Filter A*. It confirms that the two DM filter designs in *Step 4(b)* meet the same goal.

A comparison of the actual filter performance and the predicted performance is given in Fig. 11. At low frequency both agree well. However, the comparison was not made beyond 540 KHz frequency because the noise level has already been reduced to noise floor level beyond this frequency, and the comparison is meaningless. In order to verify the results though, a much smaller filter [see Fig. 12(a)] was deliberately used so that a meaningful comparison could be made. The actual performance is shown in Fig. 12(b) for CM and 12(c) for DM. The resultant comparison is shown in Fig. 12(d) and (e). From the comparison, the theoretical and the experimental results agree well below 700 KHz for both the CM and DM emission. Beyond 700 KHz, the two begin to deviate. It was found out that the deviation around 700 KHz was caused by the fact that the impedance of the 1.9 mH CM choke used in the test starts to peak and becomes capacitive around 900 KHz due to core permeability reduction and parasitic capacitance. This

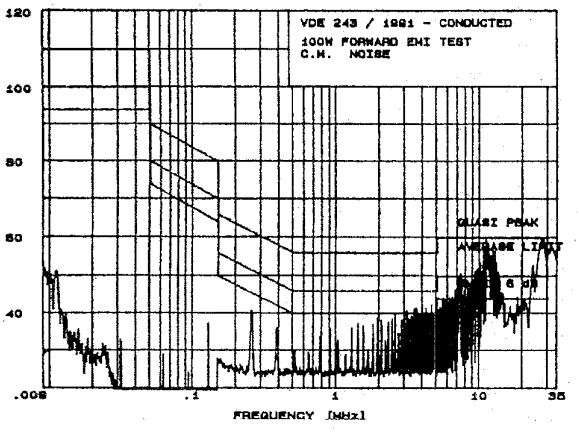

(a)

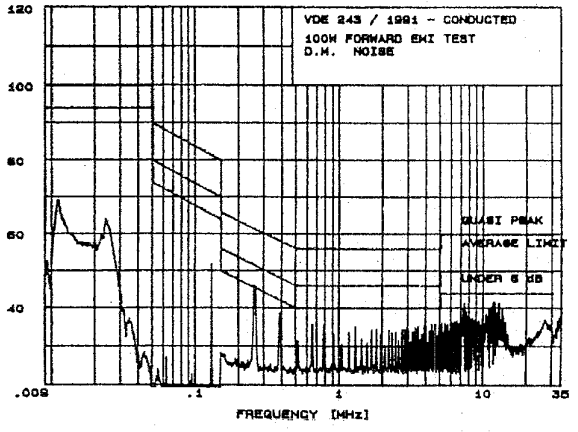

(b)

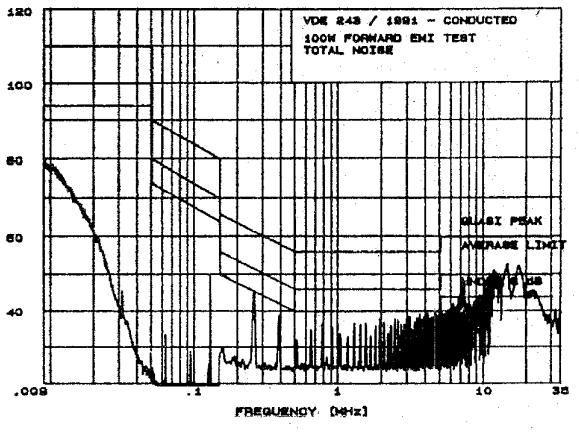

(c)

Fig. 15. (a) Measured CM noise for Example 2 when the calculated EMI filter is used. (b) Measured DM noise for Example 2 when the calculated EMI filter is used. (c) Measured total noise for Example 2 when the calculated EMI filter is used.

confirms earlier assertion that high-frequency performance is difficult to predict and can only be modified after the filter has been constructed and tested.

Example 2: Design an EMI filter for an off-line (90–260 V) forward switching power supply (130 KHz, 100 W output), as shown in Fig. 13(a), to meet a VDE limit.

Step 1: Fig. 13(b) and (c) shows the base-line CM noise V_{CM} and the base-line DM noise VDM of the tested circuit, respectively. Fig. 13(d) shows the total noise V_{Total} of the tested circuit.

Step 2: The CM attenuation requirement and the DM attenuation requirement are plotted in a log-log scale as shown in Fig. 14(a) and (b).

Step 3: From Fig.14(a) and (b), $f_{R,CM} = 14.6$ kHz and $f_{R,DM} = 13.0$ kHz

Step 4a): Use $C_y = 3300$ pF, then L_C can be calculated from (1) as 18.0 mH. Choose a CM choke with $L_C = 20$ mH. The leakage of the choke is about 240 mH from measurement.

Step 4b): Using the leakage inductance ($L_{leakage} = 240\,\mu$H) of the CM choke as L_D and (3), C_{DM} ($= C_{X1} = C_{X2}$) is calculated to be 0.625 μF, which is a practical value. So choose $C_{DM} = 0.68\,\mu$F. Fig. 15 shows the test results when the filter was used. The results agree well with the theory in the low-frequency range. To meet the high-frequency spec., modification is needed, but no effort was made in this case to resolve the high-frequency problem because it is beyond the scope of the paper.

VI. Conclusion

A practical procedure for designing the EMI filter is presented. This procedure leads to a quick filter design that at least meets the low-frequency part of design specification. Once designed and built, the filter may need slight modification to meet the high-frequency specification. This procedure facilitates the EMI filter design process and greatly reduces cut-and-trial effort.

A typical EMI filter topology is used in the illustration in the paper, and the procedure has been experimentally verified in two switching power supply applications. The same procedure can be extended to other filter topologies, but this requires further work.

References

[1] T. Guo, D. Chen, and F. C. Lee, "Separation of common-mode and differential-mode conducted EMI noise," in *Proc. High Frequency Power Conf.,* Apr. 1994, San Jose, CA.

[2] M. Nave, *Power Line Filter Design for Switched Mode Power Supplies.* Van Nostrand, 1991.

[3] L. Schneider, "Noise source equivalent circuit model for off-line converters and its use in input filter design," in *Proc. IEEE Symp.,* 1983, pp. 167–175.

[4] D. Neufeldt, "Radiation masks conducted RFI power line filtering test," *EMC Technol. Mag.,* Apr.–Jun. 1984.

[5] R. D. Middlebrook, "Input filter considerations in design and application of switching regulators," in *IEEE Ind. Applicat. Soc. Annu. Meet. Rec.,* 1976, pp. 366–382.

[6] F. S. Dos Reis, J. Sebastian, and J. Uceda, "Determination of EMI emission in power factor preregulators by design," in *IEEE PESC '94,* pp. 1117–1126.

[7] T. F. Wu, K. Siri, and C. Q. Lee, "A systematic method in designing line filters for switching regulators," in *Proc. IEEE APEC '92,* pp. 179–185.

[8] J. M. Simonelli and D. A. Torrey, "Input-filter design considerations for boost-derived high power-factor converters," in *Proc. IEEE APEC '92,* pp. 186–192.

[9] F. Lin and D. Y. Chen, "Reduction of power supply EMI emission by switching frequency modulation," in *Proc. IEEE PESC '93,* pp. 127–133.

[10] P. Caldeira, R. Liu, D. Dalal, and W. J. Gu, "Comparison of EMI performance of PWM and resonant power converters," in *Proc. IEEE PESC '93,* pp. 134–140.

Fu-Yuan Shih, for a photograph and biography, see this issue, p. 131.

Dan Y. Chen (S'72–M'75–SM'83), for a photograph and biography, see this issue, p. 131.

Yan-Pei Wu, for a photograph and biography, see this issue, p. 131.

Yie-Tone Chen (S'91–M'94), for a photograph and biography, see this issue, p. 131.